eLIFE elifesciences.org

RESEARCH ARTICLE

Reciprocal regulation among TRPV1 channels and phosphoinositide 3-kinase in response to nerve growth factor

Anastasiia Stratiievska[1], Sara Nelson[1], Eric N Senning[1†], Jonathan D Lautz[2], Stephen EP Smith[2,3], Sharona E Gordon[1]*

[1]Department of Physiology and Biophysics, University of Washington, Seattle, United States; [2]Center for Integrative Brain Research, Seattle Children's Research Institute, Seattle, United States; [3]Department of Pediatrics and Graduate Program in Neuroscience, University of Washington, Seattle, United States

Abstract Although it has been known for over a decade that the inflammatory mediator NGF sensitizes pain-receptor neurons through increased trafficking of TRPV1 channels to the plasma membrane, the mechanism by which this occurs remains mysterious. NGF activates phosphoinositide 3-kinase (PI3K), the enzyme that generates PI(3,4)P_2 and PIP_3, and PI3K activity is required for sensitization. One tantalizing hint came from the finding that the N-terminal region of TRPV1 interacts directly with PI3K. Using two-color total internal reflection fluorescence microscopy, we show that TRPV1 potentiates NGF-induced PI3K activity. A soluble TRPV1 fragment corresponding to the N-terminal Ankyrin repeats domain (ARD) was sufficient to produce this potentiation, indicating that allosteric regulation was involved. Further, other TRPV channels with conserved ARDs also potentiated NGF-induced PI3K activity. Our data demonstrate a novel reciprocal regulation of PI3K signaling by the ARD of TRPV channels.

DOI: https://doi.org/10.7554/eLife.38869.001

***For correspondence:** seg@uw.edu

Present address: †Department of Neuroscience, The University of Texas at Austin, Austin, United States

Competing interests: The authors declare that no competing interests exist.

Funding: See page 13

Received: 02 June 2018
Accepted: 06 December 2018
Published: 18 December 2018

Reviewing editor: Baron Chanda, University of Wisconsin-Madison, United States

Introduction

Although the current opioid epidemic highlights the need for improved pain therapies, in particular for pain in chronic inflammation (***Johannes et al., 2010***), too little is known about the mechanisms that mediate increased sensitivity to pain that occurs in the setting of injury and inflammation (***Ji et al., 2014***). Inflammatory hyperalgesia, the hypersensitivity to thermal, chemical, and mechanical stimuli (***Cesare and McNaughton, 1996***), can be divided in two phases, acute and chronic (***Dickenson and Sullivan, 1987***). Locally released inflammatory mediators, including growth factors, bradykinin, prostaglandins, ATP and tissue acidification (***Kozik et al., 1998***; ***Lardner, 2001***; ***Tissot et al., 1989***; ***Burnstock, 1972***), directly stimulate and sensitize nociceptive fibers of primary sensory neurons (***Cesare and McNaughton, 1996***; ***Bevan and Yeats, 1991***; ***Trebino et al., 2003***; ***Hamilton et al., 1999***; ***Mcmahon et al., 1995***).

One of the proteins that has been studied for its role in hyperalgesia is Transient Receptor Potential Vanilloid Subtype 1 (TRPV1). TRPV1 is a non-selective cation channel that is activated by a variety of noxious stimuli including heat, extracellular protons, and chemicals including capsaicin, a spicy compound in chili pepper (***Caterina et al., 1999***). TRPV1 is expressed in sensory nociceptive neurons, which are characterized by cell bodies located in the dorsal root ganglia (DRG) and trigeminal ganglia (***Caterina et al., 1999***). Sensory afferents from these neurons project to skin and internal organs, and synapse onto interneurons in the dorsal horn of the spinal cord (***Willis, 1978***). TRPV1 activation leads to sodium and calcium influx, which results in action potential generation in the sensory neuron and, ultimately, pain sensation (***Caterina et al., 1997***).

The importance of TRPV1 in inflammatory hyperalgesia was demonstrated by findings that the TRPV1 knock-out mouse showed decreased thermal pain responses and impaired inflammation-induced thermal and chemical hyperalgesia (**Caterina et al., 2000**). TRPV1 currents are enhanced during inflammation which leads to increased pain and lowered pain thresholds (**Davis et al., 2000**; **Zhang et al., 2005**; **Shu and Mendell, 1999**). TRPV1 is modulated by G-protein-coupled receptors (GPCRs) and receptor tyrosine kinases (RTKs), but the mechanisms by which these receptors modulate and sensitize TRPV1 are controversial (**Suh and Oh, 2005**; **Shu and Mendell, 1999**; **Cesare and McNaughton, 1996**).

Nerve growth factor (NGF) is one of the best studied RTK agonists involved in inflammatory hyperalgesia (**Vetter et al., 1991**). NGF acts directly on peptidergic C-fiber nociceptors (**Donnerer et al., 1992**), which express RTK receptors for NGF: Tropomyosin-receptor-kinase A (TrkA) (**Mcmahon et al., 1995**) and neurotrophin receptor $p75_{NTR}$ (**Lee et al., 1992**). NGF binding to TrkA/$p75_{NTR}$ induces receptor auto-phosphorylation and activation of downstream signaling pathways including phospholipase C (PLC), mitogen-activated protein kinase (MAPK), and Type IA phosphoinositide 3-kinase (PI3K) (**Vetter et al., 1991**; **Raffioni and Bradshaw, 1992**; **Dikic et al., 1995**). We and others have previously shown that the acute phase of NGF-induced sensitization requires activation of PI3K, which increases trafficking of TRPV1 channels to the PM (**Stein et al., 2006**; **Bonnington and McNaughton, 2003**). In chronic pain, NGF also produces changes in the protein expression of ion channels such as TRPV1 and NaV1.8 (**Ji et al., 2002**; **Thakor et al., 2009**; **Keh et al., 2008**). The acute and chronic phases of the NGF response result in increased 'gain' to painful stimuli.

Type 1A PI3K is a lipid kinase, which phosphorylates the signaling lipids Phosphatidylinositol (4) phosphate (PI4P) and Phosphatidylinositol (4,5) bisphosphate (PIP_2) into Phosphatidylinositol (3,4) bis phosphate ($PI(3,4)P_2$)and Phosphatidylinositol (3,4,5) trisphosphate (PIP_3), respectively (**Auger et al., 1989**). $PI(3,4)P_2$ and PIP_3 are signaling lipids as well, and their role in membrane trafficking and other downstream signaling is well-established (**Insall and Weiner, 2001**; **Hawkins and Stephens, 2016**). PI3K is an obligatory heterodimer that includes the catalytic p110 subunit (with α, β, and γ isoforms) and regulatory p85 subunit (with α and β isoforms) (**Hiles et al., 1992**; **Vanhaesebroeck et al., 2010**). The p85 subunit contains two Src homology 2 (SH2) domains (**Escobedo et al., 1991**), which recognize the phospho-tyrosine motif Y-X-X-M of many activated RTKs and adaptor proteins (**Songyang et al., 1993**). In the resting state, p85 inhibits the enzymatic activity of p110 via one of its SH2 domains (**Miled et al., 2007**). This autoinhibition is relieved when p85 binds to a phospho-tyrosine motif (**Miled et al., 2007**). NGF-induced PI3K activity leads to an increase in the number of TRPV1 channels at the PM (**Bonnington and McNaughton, 2003**; **Stein et al., 2006**).

We have previously shown that TRPV1 and p85 interact directly (**Stein et al., 2006**). We localized the TRPV1/p85 interaction to the N-terminal region of TRPV1 and a region including two SH2 domains of p85 (**Stein et al., 2006**). However, whether the TRPV1/p85 interaction contributes to NGF-induced trafficking of TRPV1 is unknown. Here, we further localized the functional interaction site for p85 to the region of TRPV1 N-terminus containing several conserved Ankyrin repeats (Ankyrin repeat domain (ARD)). Remarkably, we found that TRPV1 potentiated the activity of PI3K and that a soluble TRPV1 fragment corresponding to the ARD was sufficient for this potentiation. Because the ARD is structurally conserved among TRPV channels, we tested whether other TRPV channels could also potentiate NGF-induced PI3K activity. We found that TRPV2 and TRPV4 both potentiated NGF-induced PI3K activity and trafficked to the PM in response to NGF. Together, our data reveal a previously unknown reciprocal regulation among TRPV channels and PI3K. We speculate that this reciprocal regulation could be important wherever TRPV channels are co-expressed with PI3K-coupled RTKs.

Results and discussion

NGF-induced trafficking of TRPV1 channels to the PM is preceded by activation of PI3K

To study events that underlie NGF-induced trafficking of TRPV1 to the PM, we used TIRF microscopy to visualize fluorescently labeled TRPV1 (rat) (YFP-fusion, referred to as TRPV1) in transiently

transfected F-11 cells. Cells were also transfected with the NGF receptor subunits TrkA and $p75_{NTR}$ (referred to as TrkA/ $p75_{NTR}$). TIRF microscopy isolates ~ 100 nm of the cell proximal to the coverslip (***Ambrose, 1961***; ***Axelrod, 1981***), capturing the PM-proximal fluorescent signals. A change in TRPV1 fluorescence reflects a change in the number of TRPV1 channels at the PM.

We examined NGF-dependent changes in PM-associated TRPV1 before (***Figure 1A***, time point 1), during, and following (***Figure 1A***, time point 2) a 10-min exposure of the cells to NGF (100 ng/ml) via its addition to the bath (bar with gray shading in ***Figure 1B,C***). ***Figure 1A***, bottom panel shows representative TIRF images of TRPV1 fluorescence of an individual F-11 cell footprint. Consistent with previous findings (***Stein et al., 2006***), upon addition of NGF, TRPV1 levels at the PM increased, with time point two depicting the cell footprint intensity at steady state. For each cell, we normalized the mean fluorescence intensity within the footprint at each time point to the mean between 0 and 60 s prior to the application of NGF. The signal for TRPV1 for the cell in ***Figure 1A*** is shown in ***Figure 1B***, and the collected data, showing the mean and standard error of the mean, are illustrated in ***Figure 1C***.

To evaluate NGF-induced PI3K activity, we used fluorescently tagged Btk-PH and Akt-PH, PH (Pleckstrin Homology) domain probes that recognize primarily PIP_3 or both $PI(3,4)P_2$ and PIP_3, respectively (***James et al., 1996***). Btk-PH and Akt-PH are soluble proteins that localize to the cytosol at rest, when $PI(3,4)P_2/PIP_3$ levels are very low, and are recruited to the PM upon stimulation with NGF, when PI3K becomes active and generates $PI(3,4)P_2/PIP_3$ (***Hawkins et al., 2006***; ***Lemmon, 2008***). A change in PH domain probe fluorescence reflects a change in $PI(3,4)P_2/PIP_3$ concentration at the PM, thus serving as an indirect measure of PI3K activity. Because PH domain probes have been reported to interfere with PI3K signaling (***Várnai et al., 2005***), we tested whether Btk-PH and Akt-PH are compatible with NGF signaling to TRPV1. We found that Btk-PH completely abrogated NGF-induced trafficking of TRPV1 to the PM (***Figure 1—figure supplement 1***). In contrast, Akt-PH was fully compatible with NGF-induced trafficking of TRPV1 (***Figure 1***).

As an additional control, we used an orthogonal approach to evaluate the compatibility of the Akt-PH probe with NGF signaling in our cell system. Phosphorylation of the protein kinase Akt (also known as PKB) is a well-studied signaling event downstream of PI3K (***Burgering and Coffer, 1995***; ***Kohn et al., 1995***). Akt is phosphorylated in a $PI(3,4)P_2/PIP_3$-dependent manner at two sites, T308 and S473, by PDK1 (***Alessi et al., 1997***; ***Stokoe et al., 1997***; ***Frech et al., 1997***) and mTORC2, respectively (***Sarbassov et al., 2005***). Phosphorylation of Akt at these two sites leads to full activation of Akt, regulating a variety of cellular processes, including the inflammatory response to NGF (***Xu et al., 2007***; ***Sun et al., 2007***; ***Xu et al., 2011***). Therefore, we tested whether co-expression of the Akt-PH probe altered NGF-induced Akt phosphorylation. We performed western blot analysis using anti-pAKTt308, anti-pAKTs473, and anti-panAKT antibodies. ***Figure 1—figure supplement 2*** shows that NGF-induced Akt phosphorylation was preserved in cells expressing the Akt-PH probe. We therefore utilized the Akt-PH probe as a readout of PI3K activity in the remaining experiments.

We used two-color TIRF microscopy to measure PI3K activity and TRPV1 trafficking to the PM simultaneously. Treatment of cells with NGF produced an increase in plasma-membrane associated Akt-PH, indicating that $PI(3,4)P_2/PIP_3$ levels in the PM increased. The increase was relatively rapid, with kinetics determined by both PI3K activity and the affinity of Akt-PH for $PI(3,4)P_2/PIP_3$. The increased Akt-PH signal partially decreased over time even in the continued presence of NGF (***Figure 1B and C*** orange, top), possibly due to TrkA/$p75_{NTR}$ receptor internalization (***Grimes et al., 1996***; ***Ehlers et al., 1995***) and activation of phosphoinositide 3-phosphatases, e.g. PTEN (***Malek et al., 2017***). NGF treatment also increased the PM TRPV1 signal without an apparent reversal to baseline over the duration of our experiments (***Figure 1B and C*** orange, bottom). The peak levels of Akt-PH and TRPV1 for all cells, represented as the normalized intensities measured at 4–6 min (for Akt-PH) and 8–10 min (for TRPV1) after the start of NGF application, are shown in the scatterplot of ***Figure 1D***. The distributions were not normal, but skewed toward larger values. This distribution shape is characteristic of NGF-induced TRPV1 sensitization reported previously in DRG neurons (***Stein et al., 2006***; ***Bonnington and McNaughton, 2003***), indicating that our cell expression model behaves similarly to isolated DRG neurons. NGF induced a significant increase in Akt-PH levels compared to vehicle (Mean ± SEM: 1.54 ± 0.08, n = 122 compared to 1.01 ± 0.01, n = 32, Wilcoxon rank test $p = 10^{-12}$, ***Figure 1C***, top panel, orange and black symbols respectively, see also ***Figure 1—figure supplement 3***), and a significant increase in TRPV1 levels compared to vehicle (Mean ± SEM: 1.15 ± 0.02, n = 94 compared to 0.99 ± 0.01, n = 20, Wilcoxon rank test $p = 10^{-6}$;

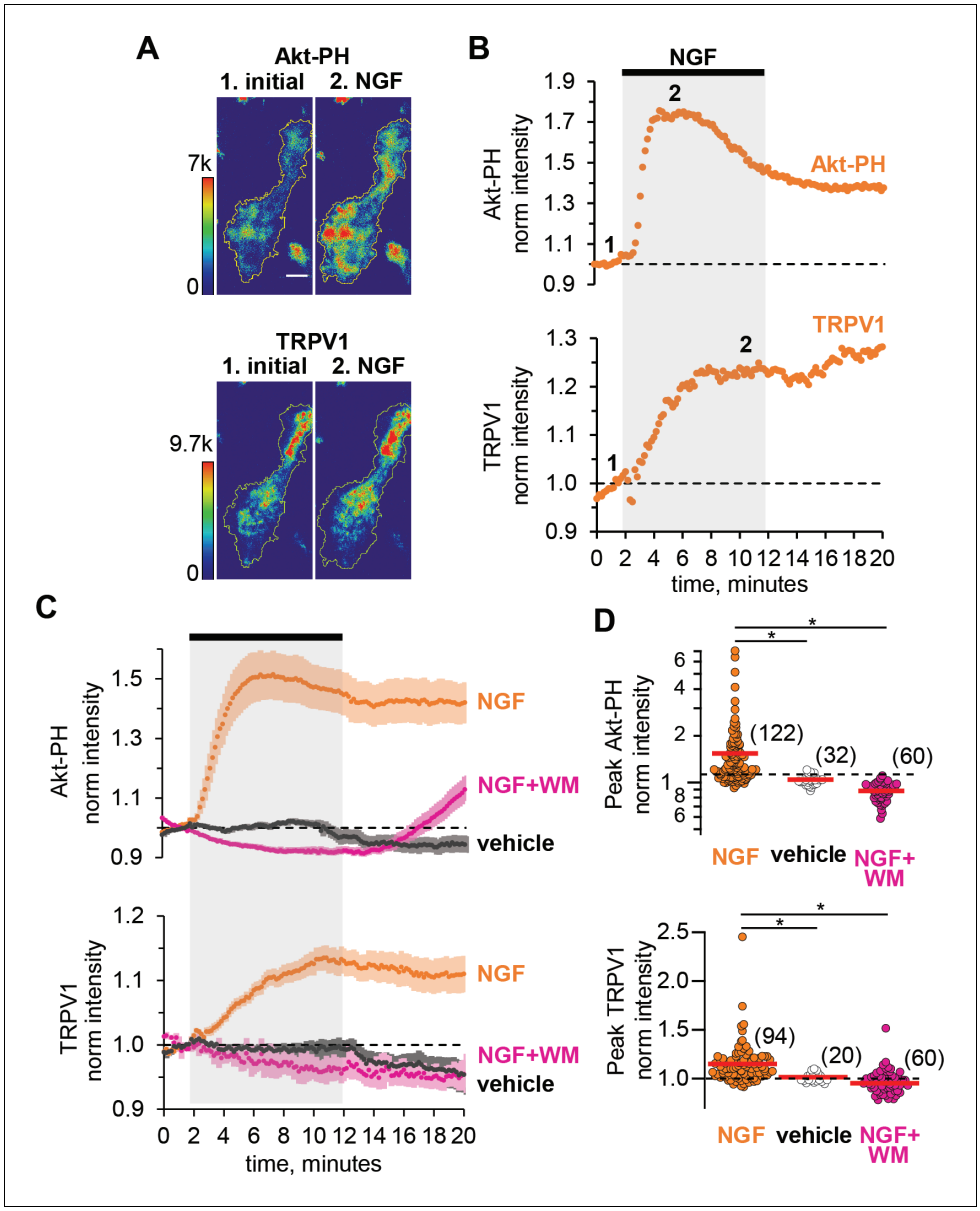

Figure 1. NGF increases PIP_3 and recruits TRPV1 to the PM. (**A**) TIRF images of a representative F-11 cell transfected with TrkA/$p75_{NTR}$, TRPV1 and Akt-PH. Images labeled one were collected before NGF application and those labeled two were collected at the plateau during NGF application, as indicated by the time points labeled in B. Scale bar is 10 μm. LUT bars represent background-subtracted pixel intensities. The yellow border represents the outline of the cell footprint. (Top) Fluorescence intensity from Akt-PH. (Bottom) Fluorescence intensity from TRPV1. (**B**) Time course of NGF-induced changes in fluorescence intensity for the cell shown in A. NGF (100 ng/mL) was applied during the times indicated by the black bar/gray shading. Intensity at each time point was measured as the mean gray value within the footprint (yellow outline in A). Data were normalized to the mean intensity values during the two minutes prior to NGF application. (**C**) And (**D**) Collected data for the group of cells tested. (**C**) Time course of NGF-induced changes in fluorescence intensity. Averaged time courses of TIRF intensity normalized as in B. Cells treated with either NGF (orange), vehicle (black) or NGF +wortmannin (NGF +WM, magenta), as indicated. TRPV1 (bottom) and Akt-PH (top). Error bars are SEM (**D**) NGF-induced change in fluorescence intensity. Cells were treated with NGF (orange), vehicle (open symbols) or NGF +wortmannin (NGF +WM, magenta), as indicated. Averaged normalized TIRF intensity during NGF application (6–8 min for Akt-PH (top) and 10–12 min for TRPV1 (bottom)). The red bars indicate the mean Akt-PH fluorescence (top) and TRPV1 fluorescence (bottom). Asterisks indicate Wilcoxon rank test significance p value < 0.001.

DOI: https://doi.org/10.7554/eLife.38869.002

Figure 1 continued on next page

Figure 1 continued

The following source data and figure supplements are available for figure 1:

Figure supplement 1. Btk-PH is not compatible with NGF signaling to TRPV1.

DOI: https://doi.org/10.7554/eLife.38869.003

Figure supplement 2. Akt-PH expression does not interfere with NGF-induced Akt phosphorylation.

DOI: https://doi.org/10.7554/eLife.38869.004

Figure supplement 2—source data 1. Full images of gel in ***Figure 1—figure supplement 2***.

DOI: https://doi.org/10.7554/eLife.38869.007

Figure supplement 3. Vehicle does not increase PIP_3 or recruit TRPV1 to PM.

DOI: https://doi.org/10.7554/eLife.38869.005

Figure supplement 4. Model for TIRF illumination and estimation of Akt-PH translocation to the PM.

DOI: https://doi.org/10.7554/eLife.38869.006

Figure supplement 4—source data 1. Depth of TIRF field and membrane translocation estimation.

DOI: https://doi.org/10.7554/eLife.38869.020

Figure 1C, bottom panel, orange and black symbols respectively, see also ***Figure 1—figure supplement 3***). Consistent with a PI3K-dependent mechanism, the NGF-induced increases in both PM-associated Akt-PH and TRPV1 were prevented by the PI3K inhibitor wortmannin (20 nM) (***Figure 1C and D***, magenta, n = 60, Mean ±SEM for Akt-PH – 0.88 ± 0.01 and for TRPV1 – 0.95 ± 0.01; Wilcoxon rank test p value for Akt-PH – 10^{-13} and for TRPV1 – 10^{-10}).

TIRF microscopy is often discussed as a method that isolates a fluorescence signal at the PM (***Axelrod, 1981***). Indeed, illumination falls off exponentially with distance from the coverslip (***Ambrose, 1961***). Nevertheless, with a typical TIRF setup such as that used for this study (see Materials and methods) ~90% of the signal comes from the cytosol (***Figure 1—figure supplement 4***, also see Materials and methods), assuming the incident light was at the critical angle and that the membrane bilayer and associated protein layer extends up to ~10 nm from the coverslip. The contamination of the TIRF signal with fluorescence from the cytosol leads to an underestimation of the change in PM-associated fluorescence from Akt-PH and TRPV1. Under our experimental conditions, we estimate that the ratio of the total fluorescence intensity measured after and before NGF application, F_{NGF}, of 1.54 translates into about a 10-fold increase in PM-associated fluorescence, R_m (***Figure 1—figure supplement 4***; see Materials and methods), although this should be considered just a rough estimate.

TRPV1 potentiates NGF-induced PI3K activity

Comparing the NGF-induced increase in Akt-PH in control cells that did not express TRPV1 to that in cells expressing TRPV1, we made an unexpected observation: TRPV1 appeared to potentiate NGF-induced PI3K activity. Comparing the time course of the NGF response in cells without TRPV1 (***Figure 2A***, blue trace) to cells expressing TRPV1 (***Figure 2A***, orange), we found a pronounced increase in Akt-PH fluorescence intensity in TRPV1-expressing cells. This increase was statistically significant, with the peak normalized Akt-PH intensity value of 1.08 ± 0.03 (n = 75) in cells without TRPV1 and 1.54 ± 0.08 (n = 122) in cells expressing TRPV1 (***Figure 2B***, Wilcoxon rank test p = 10^{-12}, see also ***Figure 2—figure supplement 1A***). Interestingly, the dynamics of NGF-induced $PI(3,4)P_2$/PIP_3-generation in the absence of TRPV1 were also different in that $PI(3,4)P_2$/PIP_3 levels were sustained. As in TRPV1-expressing cells, the NGF-induced increases in $PI(3,4)P_2$/PIP_3 levels in control cells were prevented by treatment of cells with wortmannin (***Figure 2—figure supplement 2***, Mean ± SEM: 0.81 ± 0.02, n = 53; Student's t-test p-value was 10^{-16}).

One possible cause for the potentiation of NGF-induced PI3K activity we observed in TRPV1-expressing cells could be a change in PI3K expression levels in TRPV1 vs. control cells. To determine whether this was the case, we performed western blot analysis with an anti-p85α antibody to quantify the PI3K protein levels across transfection conditions. As shown in ***Figure 2—figure supplement 3A***, expression of TRPV1 did not alter the expression level of the p85α subunit of PI3K. We quantified protein expression levels using densitometry, and normalized expression to tubulin, giving the relative expression levels shown in ***Figure 2—figure supplement 3B***. Average relative p85α expression levels were similar between non-TRPV1 expressing cells and cells expressing TRPV1 (n = 5, Student's t-test p value was 0.95). We conclude that a difference in PI3K expression in TRPV1-

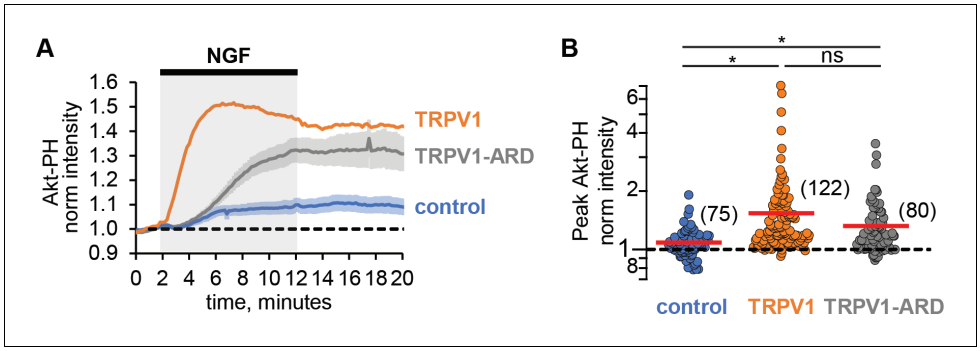

Figure 2. TRPV1-ARD is necessary and sufficient for potentiation of NGF-induced PI3K activity. (**A**) Time course of NGF-induced changes in Akt-PH fluorescence intensity. NGF (100 ng/mL) was applied during the times indicated by the black bar/gray shading. Averaged normalized TIRF intensity from cells transfected with TrkA/$p75_{NTR}$ and Akt-PH: control cells without TRPV1 (blue, n = 75), TRPV1 (orange, n = 122), or TRPV1-ARD (gray, n = 80). Traces represent the mean and error bars represent the SEM. TRPV1 data are the same as in ***Figure 1C***, error bars removed for clarity. (**B**) NGF-induced changes in Akt-PH fluorescence intensity for control cells (blue), cells expressing TRPV1 (orange data are the same as in ***Figure 1D***) and cells transfected with TRPV1-ARD (gray). Averaged normalized TIRF intensity during NGF application (6–8 min). Red bars indicate mean (see ***Table 2*** for values). Asterisks indicate significance of Holm-Bonferroni post-hoc adjusted Wilcoxon rank test p value < 0.001 (see ***Table 2*** for values).

DOI: https://doi.org/10.7554/eLife.38869.008

The following source data and figure supplements are available for figure 2:

Figure supplement 1. Representative images of NGF-induced recruitment Akt-PH and TRP channels to the PM.

DOI: https://doi.org/10.7554/eLife.38869.009

Figure supplement 2. $PI(3,4)P_2/PIP_3$ generation is diminshed by PI3K inhibitor wortmannin.

DOI: https://doi.org/10.7554/eLife.38869.010

Figure supplement 3. TRPV1 co-expression does not alter PI3K expression.

DOI: https://doi.org/10.7554/eLife.38869.011

Figure supplement 3—source data 1. Full image of gel in ***Figure 2—figure supplement 3***.

DOI: https://doi.org/10.7554/eLife.38869.012

expressing vs. control cells did not account for the observed TRPV1-induced potentiation of NGF-stimulated PI3K activity.

The ARD of TRPV1 is sufficient for potentiation of NGF-induced PI3K activity

We have previously shown that the N-terminal region of TRPV1, consisting of 110 amino acids and the ankyrin repeat domain (TRPV1-ARD), interacts directly with the p85 subunit of PI3K in yeast two-hybrid assays, co-immunoprecipitation from cells, and using recombinant fragments in vitro (***Stein et al., 2006***). We hypothesized that the TRPV1-ARD might also mediate NGF-induced potentiation of PI3K. To determine whether the ARD is sufficient for potentiation of NGF-induced PI3K activity, we expressed the ARD as a fragment and then measured NGF-induced PI3K activity. As shown in ***Figure 2A*** (gray trace), NGF induced PI3K activity that was greater in TRPV1-ARD expressing cells than in control cells (blue trace). The increase in peak Akt-PH normalized intensity was statistically significant compared to control cells, with a mean of 1.32 (±0.02, n = 80; ***Figure 2B***; Wilcoxon rank test $p = 10^{-5}$, see also ***Figure 2—figure supplement 1B***). The kinetics of this potentiation were somewhat slower with TRPV1-ARD compared to TRPV1 (***Figure 2A***, orange trace), so that Akt-PH reached steady-state levels somewhat later during NGF treatment. Nevertheless, the potentiation of NGF-induced PI3K activity by the ARD fragment was nearly as great as observed with full-length TRPV1 (Wilcoxon rank test p = 0.08). In addition, the ability of a soluble TRPV1 fragment to reconstitute potentiation suggests that the mechanism of potentiation is at least partly allosteric, involving more than just a tethering of PI3K at the membrane by TRPV1.

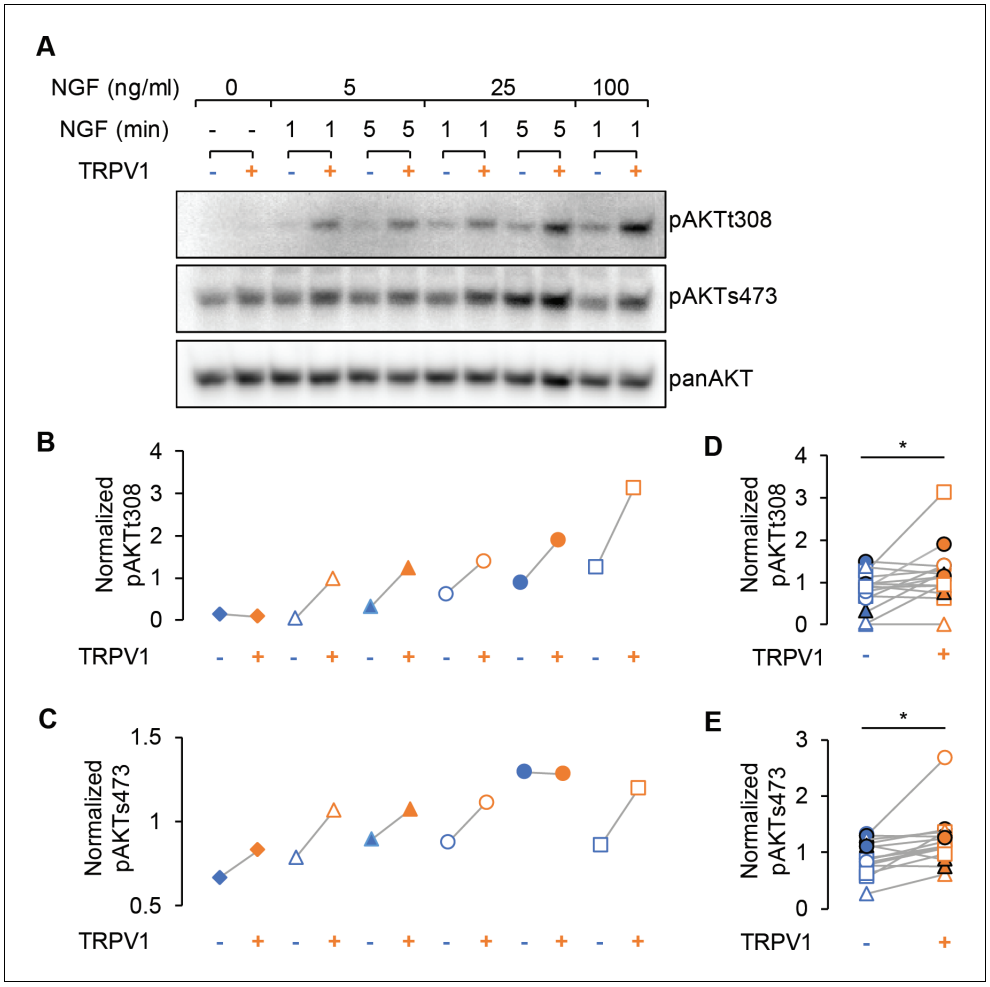

Figure 3. TRPV1 enhances NGF-induced Akt phosphorylation. (**A**) Representative immunoblot staining for analysis of Akt phosphorylation in F-11 cells transfected same as in imaging experiments. Cells were treated with indicated dose of NGF for an indicated amounts of time, lysed and loaded on SDS-PAGE. The same membrane was probed with pAKTs473, stripped and re-probed with pAKTt308 and again with panAKT antibodies (see Materials and methods). (**B**) and (**C**) Analysis of the representative blots shown in (**A**). Each band average intensity was normalized to the average of the blot and then divided by that of the corresponding lane of the panAkt blot. Akt phosphorylated at T308 (**B**) and S473 (**C**) from control cells (blue symbols) and cells expressing TRPV1 (orange symbols) treated with NGF (5, 25 or 100 ng/ml) for 1 or 5 min as indicated in (**A**). Triangles represent treatment with NGF 5 ng/ml, circles – 25 ng/m, squares – 100 ng/ml. Open symbols represent treatments for 1 min and filled symbols – 5 min. (**D**) and (**E**) Normalized phospho-Akt intensities from all indicated conditions are pooled together for the n = 3 of independent experiments. Paired Student's t-test for pAKTt308 p=0.02 and for pAKTs473 p=0.008.

DOI: https://doi.org/10.7554/eLife.38869.013

The following source data is available for figure 3:

Source data 1. Full images of gels in ***Figure 3***.

DOI: https://doi.org/10.7554/eLife.38869.016

An orthogonal PI3K assay confirms that TRPV1 potentiates NGF-induced PI3K activity and generation of $PI(3,4)P_2/PIP_3$

We used the Akt phosphorylation assay described above as an orthogonal method of examining the potentiation of NGF-induced PI3K activity in TRPV1-expressing cells. We performed western blot analysis using phospho-specific Akt antibodies, reprobing the blots with a pan Akt antibody for normalization purposes (***Figure 3A***). Because phosphorylation at T308 and S473 are differentially regulated, we used three concentrations of NGF (5, 25, and 100 ng/mL) and two incubation times (1 and 5 min). We observed increased phosphorylation at both T308 and S473 in TRPV1-expressing cells

compared to control cells for almost all trials with all three NGF concentrations and both time points (***Figure 3B,C***). The enhanced NGF-induced Akt phosphorylation was statistically significant for both T308 and S473 sites for all conditions pooled together (***Figure 3D,E***; paired Student's t-test for T308 p = 0.02 and S473 p = 0.008). Thus, TRPV1 potentiation of NGF-induced PI3K activity is sufficient to enhance $PI(3,4)P_2$ and/or PIP_3 levels to increase Akt phosphorylation.

Finally, ***Figure 3*** shows that the extent of Akt phosphorylation in unstimulated cells was indistinguishable in control vs. TRPV1-expressing cells at both S308 ($Intensity_{pAkt/pan\ Akt}$: 0.075 ± 0.004 for control and 0.076 ± 0.004 for TRPV1, Mean ± SEM, n = 3, paired Student's t-test p = 0.95) and T473 sites ($Intensity_{pAkt/pan\ Akt}$: 0.3 ± 0.24 for control and 0.23 ± 0.14 for TRPV1, Mean ± SEM, n = 3, paired Student's t-test p = 0.44), indicating that TRPV1 did not perturb the levels of $PI(3,4)P_2/PIP_3$ at rest. Importantly, we examined whether NGF-induced phosphorylation at both T308 and S473 required expression of TrkA/$p75_{NTR}$. NGF-induced phosphorylation of Akt was not observed in cells in which TrkA/$p75_{NTR}$ were not expressed (***Figure 1—figure supplement 2***). Together with the data using Akt-PH in TIRF microscopy experiments, these data indicate that NGF-induced PI3K activity is greater, and $PI(3,4)P_2/PIP_3$ production is greater, in TRPV1-expressing cells than in those that do not express TRPV1.

Potentiation of PI3K and NGF-induced trafficking are conserved among TRPV channels

The ARD of TRPV1 is highly conserved among other members of the TRPV family of ion channels (***Gaudet, 2008***). Given the sufficiency of the TRPV1 ARD in potentiation of NGF-induced PI3K activity, we postulated that reciprocal regulation among other TRPV family members and PI3K would occur as well. We examined whether other ARD-containing TRP channels, TRPV2 (rat) and TRPV4 (human) were trafficked to the plasma membrane in response to NGF. Using TRPV2 and TRPV4 fused to fluorescent proteins, we found that they were both trafficked to the PM in response to NGF compared to vehicle (Holm-Bonferroni post-hoc adjusted Wilcoxon rank test $p < 0.05$ see ***Table 1***, ***Figure 4C,D***, see also ***Figure 4—figure supplement 1*** for representative images). In addition, we found that the NGF-induced increase in Akt-PH was significantly greater in TRPV2- and TRPV4-expressing cells compared to control cells (Holm-Bonferroni post-hoc adjusted Wilcoxon rank test $p < 0.05$ see ***Table 2***, ***Figure 4A,B***). The effects of TRPV2 and TRPV4 on $PI(3,4)P_2/PIP_3$ levels were significantly smaller than those elicited by TRPV1 (Holm-Bonferroni post-hoc adjusted Wilcoxon rank test $p < 0.05$ see ***Table 2***). Further experiments would be required to determine whether the differences were due to differences in expression level, differences in the affinity of PI3K for the TRPV ARDs, or differences in the effect of each ARD on the catalytic activity of PI3K. We conclude that potentiation of NGF-induced PI3K activity and traffic to the PM in response to NGF are conserved among TRPV1, TRPV2, and TRPV4.

Increased trafficking of TRPV1 to the cell surface is essential for sensitization to noxious stimuli produced by NGF and other inflammatory mediators (***Morenilla-Palao et al., 2004***; ***Ferrandiz-Huertas et al., 2014***). Although the involvement of PI3K in NGF-induced sensitization has been known for over a decade (***Bonnington and McNaughton, 2003***; ***Stein et al., 2006***), the role, if any,

Table 1. Normalized TRP channel fluorescence intensities measured during NGF application for all discussed conditions.

The number of cells in the data set collected over at least three different experiments is given by n. Non-adjusted Wilcoxon rank test two tail p values was performed for pairwise comparisons as indicated.

	NGF Mean ± SEM	N=	TRPV1	Vehicle
TRPV1	1.15 ± 0.02	94	-	-
vehicle	1.01 ± 0.01	20	10^{-6}	-
TRPV2	1.12 ± 0.02	62	0.24	0.002
TRPV4	1.11 ± 0.02	48	0.13	0.002

DOI: https://doi.org/10.7554/eLife.38869.017

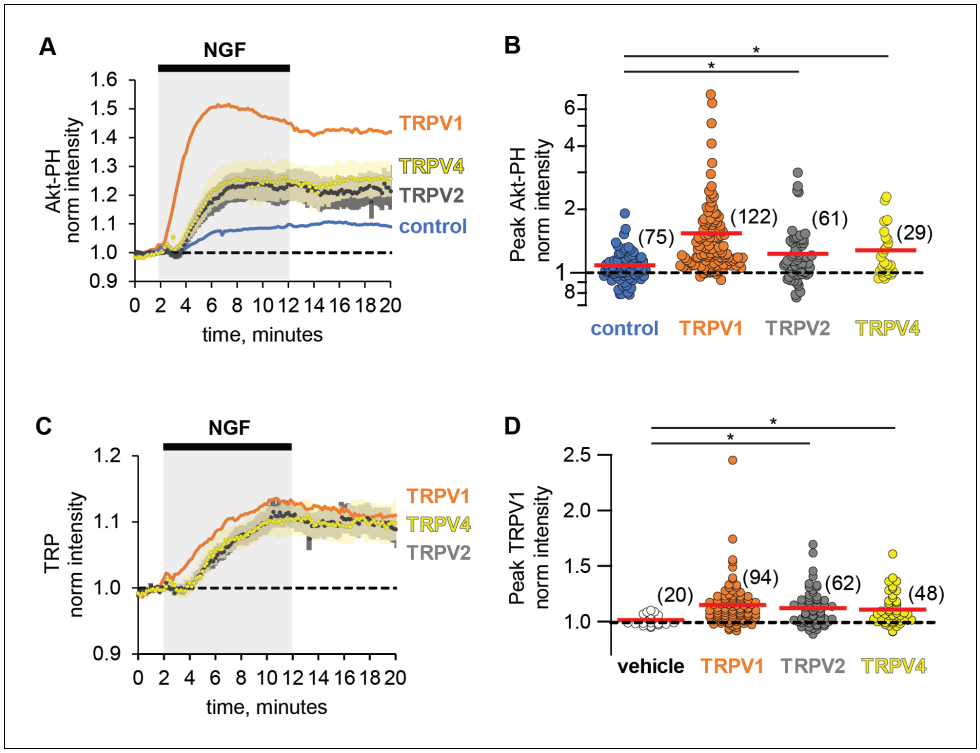

Figure 4. Potentiation of PI3K and NGF-induced trafficking are conserved among TRPV channels. Time course of NGF-induced changes in fluorescence intensity. NGF (100 ng/mL) was applied during the times indicated by the black bar/gray shading. Traces represent the mean, error bars are SEM. Control and TRPV1 data same as in ***Figure 2*** with error bars removed for clarity. (**A**) Averaged normalized TIRF intensity of Akt-PH from cells transfected with TrkA/$p75_{NTR}$ and Akt-PH and: (**A**) no channel (control; blue; n = 75); TRPV1 (orange; n = 122); TRPV2 (black; n = 61); TRPV4 (yellow; n = 29). (**B**) Averaged normalized Akt-PH intensity during NGF application (6–8 min). The red bars indicate the mean. Asterisks indicate significance (Holm-Bonferroni post-hoc adjusted Wilcoxon rank test $p < 0.05$, see ***Table 2*** for values). (**C**) Averaged normalized TIRF intensity of individual TRP channels. Color scheme as in (**A**) with the cell numbers as follows: TRPV1 (n = 94); TRPV2 (n = 62); TRPV4 (n = 48). (**D**). Averaged normalized TRP channel intensity during NGF application (8–10 min). The red bars indicate the mean. Asterisks indicate significance (Holm-Bonferroni post-hoc adjusted Wilcoxon rank test $p < 0.05$, see ***Table 1*** for values).

DOI: https://doi.org/10.7554/eLife.38869.014

The following figure supplement is available for figure 4:

Figure supplement 1. Representative images of NGF-induced recruitment Akt-PH and TRP channels to the PM.

DOI: https://doi.org/10.7554/eLife.38869.015

of direct binding of TRPV1 and PI3K was unclear. Here, we show that ARD region of TRPV1 that binds PI3K is sufficient to potentiate NGF-induced PI3K activity. Although it is possible that TRPV1 inhibition of the $PI(3,4)P_2/PIP_3$ phosphatase PTEN (***Malek et al., 2017***) could contribute to TRPV1 potentiation of NGF-induced increases in $PI(3,4)P_2/PIP_3$ levels, this and other more complex models are not needed to explain our data. In addition, whereas the present work does not rule out that the potentiation of PI3K we describe requires an effector that mediates signaling between the TRPV1 ARD and PI3K, we favor a simpler model in which the previously described direct interaction between TRPV1 and PI3K mediates the signaling. We speculate that, without TRPV1 potentiation of PI3K, NGF signaling would not produce sufficient $PI(3,4)P_2/PIP_3$ to promote channel trafficking during inflammation. Future studies that decouple potentiation of PI3K activity from the expression of TRPV channels will be needed to determine whether the reciprocal regulation between ARD-containing TRPV channels and PI3K serves an obligate role in channel sensitization.

Is reciprocal regulation among TRPV channels and PI3K relevant beyond pain signaling? TRPV channels have been proposed to be involved in RTK/PI3K signaling in a variety of cell types

Table 2. Normalized Akt-PH fluorescence intensities measured during NGF application for all discussed conditions.
The number of cells in the data set collected over at least three different experiments is given by n. Non-adjusted Wilcoxon rank test two tail p values for pairwise comparisons as indicated.

Akt-PH from	NGF Mean ± SEM	N=	Control	TRPV1
control	1.08 ± 0.03	75	-	-
TRPV1	1.54 ± 0.8	122	10^{-12}	-
TRPV1-ARD	1.32 ± 0.2	80	10^{-5}	0.08
TRPV2	1.23 ± 0.18	61	0.04	0.0002
TRPV4	1.28 ± 0.14	29	0.02	0.02

DOI: https://doi.org/10.7554/eLife.38869.018

(***Reichhart et al., 2015***; ***Katanosaka et al., 2014***; ***Jie et al., 2015***; ***Sharma et al., 2017***). For example, TRPV2 is co-expressed in muscle cells with the insulin like growth factor receptor (IGFR) and is known to be important in muscle loss during muscular dystrophy (***Iwata et al., 2003***). The mechanism is believed to involve IGFR activation leading to increased trafficking of TRPV2 to the sarcolemma, Ca^{2+} overload/cytotoxicity, and cell death (***Iwata et al., 2003***; ***Perálvarez-Marín et al., 2013***; ***Katanosaka et al., 2014***). Whether TRPV2 potentiates IGF-induced PI3K activity remains to be determined. The co-expression of TRPV channels with RTK/PI3K in other tissues, including nerve (TRPV1/NGF) (***Tanaka et al., 2016***), muscle (TRPV2/IGF) (***Katanosaka et al., 2014***) and lung (TRPV4/TGFβ1) (***Rahaman et al., 2014***) raises the question of whether reciprocal regulation among TRPV channels and PI3K plays a role in RTK signaling in cell development, motility, and/or pathology.

Materials and methods

TIRF microscopy and analysis

For imaging, we used an inverted microscope (NIKON Ti-E) equipped for total internal fluorescence (TIRF) imaging with a 60x objective (NA 1.49). Glass coverslips with adherent cells were placed in a custom-made chamber. The chamber volume (~1 ml) was exchanged using a gravity-driven perfusion system. Cells were acclimated to flow for at least 15 min prior to NGF application. Akt-PH fused to Cyan Fluorescent Protein (CFP) was imaged using excitation from a 447 nm laser and a 480/40 emission filter. TRPV1 fused to Yellow Fluorescent Protein (YFP) was imaged using the 514 nm line of an argon laser and a 530 long-pass emission filter. Time-lapse images were obtained by taking consecutive CFP and YFP images every 10 s. Movies were then processed using ImageJ software (NIH) (***Rasband, 1997***). Regions of interest (ROI) were drawn around the footprint of individual cells and the average ROI pixel intensity was measured. Measurements were analyzed using Excel 2013 (Microsoft Corporation), by subtracting the background ROI intensity from the intensity of each cell ROI. Traces were normalized by the average intensity during the 1-min time period prior to NGF application.

Depth of TIRF field and membrane translocation estimation

Because $PI(3,4)P_2/PIP_3$ levels reported by the Akt-PH fluorescence measured with TIRF microscopy include significant contamination from free Akt-PH in the cytosol, we used the characteristic decay of TIRF illumination to estimate the fraction of our signal due to Akt-PH bound to the membrane. We first estimated the fraction of the illumination at the membrane in resting cells, assuming that free Akt-PH is homogeneously distributed throughout the evanescent field. After stimulation with NGF, we then used this fraction of illumination at the membrane to determine the fraction of the emission light originating from this region. The estimation approach used below was not used to quantitatively evaluate our data. Rather, it demonstrates the general issue of cytosolic contamination causing underestimation of changes in membrane-associated fluorescence even when using TIRF microscopy.

The depth of the TIRF field was estimated as described in the literature (***Axelrod, 1981***; ***Mattheyses and Axelrod, 2006***). Briefly, when laser light goes through the interface between a

coverslip with refractive index n_2 and saline solution with refractive index n_1, it experiences total internal reflection at angles less than the critical incidence angle, θ_c, given by

$$\theta_c = sin^{-1}\left(\frac{n_1}{n_3}\right)$$

The characteristic depth of the illuminated field d is described by

$$d = \frac{\lambda_0}{4\pi n_3}\left(sin^2\theta - sin^2\theta_c\right)^{-\frac{1}{2}}$$

where λ_0 is laser wavelength. The illumination decay τ, depends on depth of field as follows:

$$\tau = \frac{1}{d}$$

TIRF illumination intensity, I, is described in terms of distance from the coverslip, h, by

$$I = e^{-\tau h}$$

For simplicity, we measured the distance h in 'layers', with the depth of each layer corresponding to physical size of Akt-PH, which was estimated to be approximately 10 nm based on the sum of longest dimensions of Akt-PH and GFP in their respective crystal structures (PDB ID: 1UNQ and 1GFL). We solved for TIRF illumination intensity using the following values for our system: refractive indexes of solution n_1 = 1.33 and coverslip n_3 = 1.53, critical incidence angle θ_C = 60.8 degrees. The laser wavelength used in our experiments was λ_0 = 447 nm, and the experimental angle of incidence was θ_{exp} = 63 degrees. This produces a characteristic depth of d_{63} = 127 nm and an illumination decay of τ_{63} = 0.008 nm^{-1}. We plot TIRF illumination intensity over distance in molecular layers and nanometers in ***Figure 1—figure supplement 4***.

The values determined above allow us to estimate the contributions to our TIRF signal from the membrane vs. the cytosol. According to our calculation, the TIRF illumination intensity approaches 0 at around 500 nm, or layer h_{49}. We consider the membrane and associated proteins to reside in layer h_0. Under these conditions, at rest, 5% of total recorded TIRF fluorescence arises from h_0, with the remainder originating from h_1-h_{49}. At rest, we assume that Akt-PH molecules are distributed evenly throughout layers h_0-h_{49}, with no Akt-PH bound to the membrane because the concentration of PI(3,4)P_2/PIP_3 in the PM is negligible at rest. Total fluorescence intensity measured before NGF application, $F_{initial}$, depends on m, the number of molecules per layer at rest, B, the brightness of a single molecule of CFP, and TIRF illumination intensity, I:

$$F_{initial} = \mathrm{B}*\sum_{0}^{49} mI_i$$

Normalizing our time traces to $F_{initial}$, sets $F_{initial}$ = 1. We solved for m numerically using Excel (Microsoft, Redmond, WA; see ***Figure 1—figure supplement 4—source data 1***), and determined a value of 0.08. We assumed a fixed number of molecules in the field and that the only NGF-induced change was a redistribution of molecules among layers. The total fluorescence intensity measured after NGF application, F_{NGF}, will reflect the redistribution of Δm molecules between membrane layer h_0 and all layers h_0-h_{49}, with free Akt-PH homogeneously distributed among these layers. Therefore, F_{NGF} is a sum of fluorescence intensities of the number of bound molecules in the membrane layer h_0 and the free molecules in layers h_1-h_{49}:

$$F_{NGF} = \mathrm{B}*\left[(\Delta m)I_0 + \sum_{0}^{49}\left(m - \frac{\Delta m}{50}\right)I_i\right]$$

We solved for Δm using Excel, constraining F_{NGF} to the values we measured for control and TRPV1-expressing cells (data listed in the table in ***Figure 1—figure supplement 4B***). Finally, we estimated the NGF-induced change in Akt-PH bound to the membrane as R_m, the ratio of molecules in h_0 after NGF to that before NGF:

$$R_m = \frac{(m+\Delta m)I_0}{mI_0}$$

We compared R_m values to the F_{NGF} values listed in the table ***Figure 1—figure supplement 4B***. For example, in cells expressing TRPV1, F_{NGF} of 1.54 led to 10 times more membrane-associated Akt-PH molecules. Note, that if we instead allow the number of molecules in cytosolic layers to remain constant as m_0 increases with NGF treatment, we calculate an R_m value of 8, very similar to the value of 10 obtained with redistribution of a fixed number of molecules across all layers. Both of these scenarios are independent of the initial Akt-PH fluorescence intensity in a given cell.

Cell culture/transfection/ DNA constructs/solutions

F-11 cells (a gift from M.C. Fishman, Massachusetts General Hospital, Boston, MA; (***Francel et al., 1987***)) were cultured at 37°C, 5% CO_2 in Ham's F-12 Nutrient Mixture (#11765–054; Gibco) supplemented with 20% fetal bovine serum (#26140–079; Gibco, Grand Island, NY), HAT supplement (100 µM sodium hypoxanthine, 400 nM aminopterin, 16 µM thymidine; #21060–017; Gibco), and penicillin/streptomycin (#17-602E, Lonza, Switzerland). F-11 cells were tested for mycoplasma contamination using Universal Mycoplasma Detection Kit (# ATCC 30–1012K, ATCC, Manassas, VA) and found to be free of contamination. F-11 cells for imaging experiments were plated on Poly-Lysine (#P1274, Sigma, St. Louis, MO) coated 0.15 mm x 25 mm coverslips (#64–0715 (CS-25R15), Warner Instruments, Hamden, CT) in a six-well plate. Cells were transfected with Lipofectamine 2000 (4 µl/well, Invitrogen, Grand Island, NY) reagent using 1–3 µg of cDNA per well. 24 hr post-transfection, media was replaced with HEPES-buffered saline (HBR, double deionized water and in mM: 140 NaCl, 4 KCl, 1 $MgCl_2$, 1.8 $CaCl_2$, 10 HEPES (free acid) and five glucose) for at least 2 hr prior to the imaging. During experiments, cells were treated with 100 ng/ml NGF 2.5S (#13257–019, Sigma), vehicle (HBR) or 20 nM wortmannin (Sigma W1628).

TRPV1-cYFP (rat) (***Ufret-Vincenty et al., 2015***), TRPV1-ARD-ctagRFP (rat), TRPV2-cYFP (rat) (***Mercado et al., 2010***) DNA constructs were made in the pcDNA3 vector (Invitrogen), where '-n' or '-c' indicates that the fluorescent protein is on the N- or C-terminus, respectively. TRPV4-EGFP (human) in pEGFP was obtained from Dr. Tim Plant (Charite-Universitatsmedizine, Berlin) (***Strotmann et al., 2003***). TrkA (rat) in the pcCMV5 vector and $p75_{NTR}$ (rat) in the pcDNA3 vector were obtained from Dr. Mark Bothwell (University of Washington, Seattle). PH-Akt-cCerulean in the pcDNA3-k vector was made based on the construct in the pHR vector from Dr. Orion Weiner's Lab (***Toettcher et al., 2011***). The function of the ion channels tested were confirmed using Ca^{2+} imaging and/or patch clamp electrophysiology (data not shown).

Western blotting

For detection of relative expression of PI3K p85α subunit, cells were transfected as described above for imaging experiments. 24 hr after transfection, cells were scraped off the bottom of 10 cm plates, washed with Phosphate Buffered Saline (PBS) 4 times and homogenized in Lysis buffer (1% Triton 25 mM Tris-HCl, 150 mM NaCl, 1 mM EDTA, pH 7.4) for 2 hr with mixing at 4°C. Lysates were spun down at 14000 rpm for 30 min at 4°C to remove the cell nuclei and debris. Cleared lysates were mixed with Laemmli 2x SDS sample buffer (#161–0737, Bio-Rad, Hercules, CA), boiled for 10 min and subjected to SDS PAGE to separate proteins by size. Gels were then transferred onto the PDVF membrane using Trans-Blot SD semi-dry transfer cell (Bio-Rad) at 15 V for 50 min. Membranes were blocked in 5% BSA Tris-Buffered Saline, 0.1% Tween (TBS-T) for 1 hr and probed with primary antibody for 1 hr at RT. Next, membranes were washed 6x times with TBS-T and probed with secondary antibodies conjugated with Horse Radish Peroxidase (HRP) for 1 hr. After another set of 6 washes membranes were developed by addition of the SuperSignal West Femto HRP substrate (#34096, Thermo, Grand Island, NY) and imaged using CCD camera-enabled imager. For quantification, blot images were analyzed in ImageJ. ROIs of the same size were drawn around the bands for p85 and tubulin, then mean pixel intensity was measured. Mean p85 intensities were normalized by dividing by mean tubulin intensities and plotted in ***Figure 2—figure supplement 3***. Experiments were repeated with n = 5 independent samples. Primary antibodies used were: anti-PI3K (alpha) polyclonal (#06–497 (newer Cat#ABS234), Upstate/Millipore, Burlington, MA) at 1:600 dilution; β Tubulin (G-8) (#sc-55529, Santa Cruz, Dallas, TX) at 1:200 dilution. Secondary antibodies used: Anti-Rabbit

IgG (#074–1506, KPL/SeraCare Life Sciences, Milford, MA) at 1:30,000 dilution; Anti-Mouse IgG (#NA931, Amersham/GE Healthcare Life Sciences, United Kingdom) at 1:30,000 dilution.

For detection of phosphorylated Akt, cells plated in six-well plates were treated for the indicated amount of time (***Figure 3***, ***Figure 1—figure supplement 2***) in the CO_2 incubator at 37˚C. Immediately after treatment, wells were aspirated and scraped in ice-cold lysis buffer (H_2O, TBS, 1% NP-40, 5 mM NaF, 5 mM Na_3VO_4 with added Protease inhibitors (#P8340, Sigma) and Phosphatase Inhibitor Cocktail 2 (#P5726, Sigma). After incubation on ice for 15 min, lysates were cleared by centrifugation at 15 k g for 15 min at 4˚C. Protein contents of cleared lysates were measured using the BCA assay (#23225 Pierce) according to manufacturer's protocol. Volumes of lysates were adjusted according to these measurements and subjected to SDS-PAGE. Gels were transferred onto PVDF membranes using wet-transfer. Membranes were blocked in TBS-T with 5% milk for 1 hr and incubated overnight at 4˚C with one of the following primary antibodies: pAKTs473 clone D9E (#4060, Cell Signaling), pAKTt308 clone 244F9 (#4056, Cell Signaling) . Further procedures were as indicated in the previous paragraph. After development membranes were stripped using Pierce Restore Western Blot stripping buffer (#21059, Thermo Fisher), reprobed with the other anti-phospho-AKT antibody and then stripped and re-probed with panAKT clone 40D4 (#2920, Cell Signaling) antibody at 1:2500 dilution. Data was normalized by diving the average intensity of a band by the average intensity of a blot and then dividing by that of a pan-Akt blot (***Figure 3***).

Acknowledgements

We thank Mika Munari, Gilbert Martinez, Mark Bothwell, Bertil Hille, William Zagotta, Shao-En Ong, Tamara Rosenbaum and Gaby Bergollo for helpful discussions. We are grateful to the following individuals for providing cDNA constructs: Dr. Tim Plant (Charite-Universitatsmedizine, Berlin) for TRPV4; Dr. Mark Bothwell (University of Washington, Seattle) for TrkA and $p75_{NTR}$; and Dr. Orion Weiner (UCSF) for PH-Akt.

Research reported in this publication was supported by the National Eye Institute of the National Institutes of Health under award numbers R01EY017564 (to SEG), by the National Institute of General Medical Sciences of the National Institutes of Health under award numbers R01GM100718 and R01GM125351 (to SEG), by the National Institute of Mental Health under award number R01MH113545 (to SEPS), by the National Institute of Biomedical Imaging and Bioengineering of the National Institutes of Health under award number T32EB001650 (to AS), by the following additional awards from the National Institutes of Health: S10RR025429, P30DK017047, and P30EY001730. and by a Royalty Research Fund Award from the University of Washington (to SEG). The content is solely the responsibility of the authors and does not necessarily represent the official views of the National Institutes of Health. The authors declare no competing financial interests.

Additional information

Funding

Funder	Grant reference number	Author
National Eye Institute	R01EY017564	Sharona E Gordon
National Institute of General Medical Sciences	R01GM100718	Sharona E Gordon
National Institute of General Medical Sciences	R01GM125351	Sharona E Gordon
University of Washington	Royalty Research Fund	Sharona E Gordon
National Institute of Mental Health	R01MH113545	Stephen EP Smith
National Institute of Biomedical Imaging and Bioengineering	T32EB001650	Anastasiia Stratiievska
National Institutes of Health	S10RR025429	Sharona E Gordon
National Institutes of Health	P30DK017047	Sharona E Gordon

National Institutes of Health	P30EY001730	Sharona E Gordon

The funders had no role in study design, data collection and interpretation, or the decision to submit the work for publication.

Author contributions

Anastasiia Stratiievska, Conceptualization, Formal analysis, Investigation, Methodology, Writing—original draft, Writing—review and editing; Sara Nelson, Investigation, Methodology; Eric N Senning, Stephen EP Smith, Conceptualization, Writing—review and editing; Jonathan D Lautz, Investigation, Methodology, Writing—review and editing; Sharona E Gordon, Conceptualization, Formal analysis, Funding acquisition, Investigation, Methodology, Writing—original draft, Writing—review and editing

Author ORCIDs

Anastasiia Stratiievska http://orcid.org/0000-0002-5523-0773
Sharona E Gordon http://orcid.org/0000-0002-0914-3361

Decision letter and Author response

Decision letter https://doi.org/10.7554/eLife.38869.023
Author response https://doi.org/10.7554/eLife.38869.024

Additional files

Supplementary files

- Source data 1. Source data from figures. Excel file containing source data from the figures as indicated. The name of Excel sheet corresponds to the figure to which it is related

DOI: https://doi.org/10.7554/eLife.38869.019

- Transparent reporting form

DOI: https://doi.org/10.7554/eLife.38869.021

Data availability

All data generated or analysed during this study are included in the manuscript and supporting files.

References

Alessi DR, James SR, Downes CP, Holmes AB, Gaffney PR, Reese CB, Cohen P. 1997. Characterization of a 3-phosphoinositide-dependent protein kinase which phosphorylates and activates protein kinase Balpha. *Current Biology* **7**:261–269. DOI: https://doi.org/10.1016/S0960-9822(06)00122-9, PMID: 9094314

Ambrose EJ. 1961. The movements of fibrocytes. *Experimental Cell Research* **8**:54–73. DOI: https://doi.org/10.1016/0014-4827(61)90340-8, PMID: 13682921

Auger KR, Carpenter CL, Cantley LC, Varticovski L. 1989. Phosphatidylinositol 3-kinase and its novel product, phosphatidylinositol 3-phosphate, are present in Saccharomyces cerevisiae. *The Journal of Biological Chemistry* **264**:20181–20184. PMID: 2555343

Axelrod D. 1981. Cell-substrate contacts illuminated by total internal reflection fluorescence. *The Journal of Cell Biology* **89**:141–145. DOI: https://doi.org/10.1083/jcb.89.1.141, PMID: 7014571

Bevan S, Yeats J. 1991. Protons activate a cation conductance in a sub-population of rat dorsal root ganglion neurones. *The Journal of Physiology* **433**:145–161. DOI: https://doi.org/10.1113/jphysiol.1991.sp018419, PMID: 1726795

Bonnington JK, McNaughton PA. 2003. Signalling pathways involved in the sensitisation of mouse nociceptive neurones by nerve growth factor. *The Journal of Physiology* **551**:433–446. DOI: https://doi.org/10.1113/jphysiol.2003.039990, PMID: 12815188

Burgering BM, Coffer PJ. 1995. Protein kinase B (c-Akt) in phosphatidylinositol-3-OH kinase signal transduction. *Nature* **376**:599–602. DOI: https://doi.org/10.1038/376599a0, PMID: 7637810

Burnstock G. 1972. Purinergic nerves. *Pharmacological Reviews* **24**:509–581. PMID: 4404211

Caterina MJ, Schumacher MA, Tominaga M, Rosen TA, Levine JD, Julius D. 1997. The capsaicin receptor: a heat-activated ion channel in the pain pathway. *Nature* **389**:816–824. DOI: https://doi.org/10.1038/39807, PMID: 9349813

Caterina MJ, Rosen TA, Tominaga M, Brake AJ, Julius D. 1999. A capsaicin-receptor homologue with a high threshold for noxious heat. *Nature* **398**:436–441. DOI: https://doi.org/10.1038/18906, PMID: 10201375

Caterina MJ, Leffler A, Malmberg AB, Martin WJ, Trafton J, Petersen-Zeitz KR, Koltzenburg M, Basbaum AI, Julius D. 2000. Impaired nociception and pain sensation in mice lacking the capsaicin receptor. *Science* **288**: 306–313. DOI: https://doi.org/10.1126/science.288.5464.306, PMID: 10764638

Cesare P, McNaughton P. 1996. A novel heat-activated current in nociceptive neurons and its sensitization by bradykinin. *PNAS* **93**:15435–15439. DOI: https://doi.org/10.1073/pnas.93.26.15435, PMID: 8986829

Davis JB, Gray J, Gunthorpe MJ, Hatcher JP, Davey PT, Overend P, Harries MH, Latcham J, Clapham C, Atkinson K, Hughes SA, Rance K, Grau E, Harper AJ, Pugh PL, Rogers DC, Bingham S, Randall A, Sheardown SA. 2000. Vanilloid receptor-1 is essential for inflammatory thermal hyperalgesia. *Nature* **405**:183–187. DOI: https://doi.org/10.1038/35012076, PMID: 10821274

Dickenson AH, Sullivan AF. 1987. Subcutaneous formalin-induced activity of dorsal horn neurones in the rat: differential response to an intrathecal opiate administered pre or post formalin. *Pain* **30**:349–360. DOI: https://doi.org/10.1016/0304-3959(87)90023-6, PMID: 3670880

Dikic I, Batzer AG, Blaikie P, Obermeier A, Ullrich A, Schlessinger J, Margolis B. 1995. Shc binding to nerve growth factor receptor is mediated by the phosphotyrosine interaction domain. *Journal of Biological Chemistry* **270**:15125–15129. DOI: https://doi.org/10.1074/jbc.270.25.15125, PMID: 7541035

Donnerer J, Schuligoi R, Stein C. 1992. Increased content and transport of substance P and calcitonin gene-related peptide in sensory nerves innervating inflamed tissue: evidence for a regulatory function of nerve growth factor in vivo. *Neuroscience* **49**:693–698. DOI: https://doi.org/10.1016/0306-4522(92)90237-V, PMID: 1380138

Ehlers MD, Kaplan DR, Price DL, Koliatsos VE. 1995. NGF-stimulated retrograde transport of trkA in the mammalian nervous system. *The Journal of Cell Biology* **130**:149–156. DOI: https://doi.org/10.1083/jcb.130.1.149, PMID: 7540615

Escobedo JA, Navankasattusas S, Kavanaugh WM, Milfay D, Fried VA, Williams LT. 1991. cDNA cloning of a novel 85 kd protein that has SH2 domains and regulates binding of PI3-kinase to the PDGF beta-receptor. *Cell* **65**:75–82. DOI: https://doi.org/10.1016/0092-8674(91)90409-R, PMID: 1849460

Ferrandiz-Huertas C, Mathivanan S, Wolf CJ, Devesa I, Ferrer-Montiel A. 2014. Trafficking of ThermoTRP Channels. *Membranes* **4**:525–564. DOI: https://doi.org/10.3390/membranes4030525, PMID: 25257900

Francel PC, Miller RJ, Dawson G. 1987. Modulation of bradykinin-induced inositol trisphosphate release in a novel neuroblastoma x dorsal root ganglion sensory neuron cell line (F-11). *Journal of Neurochemistry* **48**:1632–1639. DOI: https://doi.org/10.1111/j.1471-4159.1987.tb05712.x, PMID: 3494104

Frech M, Andjelkovic M, Ingley E, Reddy KK, Falck JR, Hemmings BA. 1997. High affinity binding of inositol phosphates and phosphoinositides to the pleckstrin homology domain of RAC/protein kinase B and their influence on kinase activity. *Journal of Biological Chemistry* **272**:8474–8481. DOI: https://doi.org/10.1074/jbc.272.13.8474, PMID: 9079675

Gaudet R. 2008. A primer on ankyrin repeat function in TRP channels and beyond. *Molecular BioSystems* **4**:372–379. DOI: https://doi.org/10.1039/b801481g, PMID: 18414734

Grimes ML, Zhou J, Beattie EC, Yuen EC, Hall DE, Valletta JS, Topp KS, LaVail JH, Bunnett NW, Mobley WC. 1996. Endocytosis of activated TrkA: evidence that nerve growth factor induces formation of signaling endosomes. *The Journal of Neuroscience* **16**:7950–7964. DOI: https://doi.org/10.1523/JNEUROSCI.16-24-07950.1996, PMID: 8987823

Hamilton SG, Wade A, McMahon SB. 1999. The effects of inflammation and inflammatory mediators on nociceptive behaviour induced by ATP analogues in the rat. *British Journal of Pharmacology* **126**:326–332. DOI: https://doi.org/10.1038/sj.bjp.0702258, PMID: 10051152

Hawkins PT, Anderson KE, Davidson K, Stephens LR. 2006. Signalling through Class I PI3Ks in mammalian cells. *Biochemical Society Transactions* **34**:647–662. DOI: https://doi.org/10.1042/BST0340647, PMID: 17052169

Hawkins PT, Stephens LR. 2016. Emerging evidence of signalling roles for PI(3,4)P2 in Class I and II PI3K-regulated pathways. *Biochemical Society Transactions* **44**:307–314. DOI: https://doi.org/10.1042/BST20150248, PMID: 26862220

Hiles ID, Otsu M, Volinia S, Fry MJ, Gout I, Dhand R, Panayotou G, Ruiz-Larrea F, Thompson A, Totty NF. 1992. Phosphatidylinositol 3-kinase: structure and expression of the 110 kd catalytic subunit. *Cell* **70**:419–429. DOI: https://doi.org/10.1016/0092-8674(92)90166-A, PMID: 1322797

Insall RH, Weiner OD. 2001. PIP3, PIP2 Complex Roles at the Cell Surface. *Cell* **1**. DOI: https://doi.org/10.1016/S0092-8674(00)80696-0

Iwata Y, Katanosaka Y, Arai Y, Komamura K, Miyatake K, Shigekawa M. 2003. A novel mechanism of myocyte degeneration involving the Ca2+-permeable growth factor-regulated channel. *The Journal of Cell Biology* **161**: 957–967. DOI: https://doi.org/10.1083/jcb.200301101, PMID: 12796481

James SR, Downes CP, Gigg R, Grove SJ, Holmes AB, Alessi DR. 1996. Specific binding of the Akt-1 protein kinase to phosphatidylinositol 3,4,5-trisphosphate without subsequent activation. *Biochemical Journal* **315**:709–713. DOI: https://doi.org/10.1042/bj3150709, PMID: 8645147

Ji RR, Samad TA, Jin SX, Schmoll R, Woolf CJ. 2002. p38 MAPK activation by NGF in primary sensory neurons after inflammation increases TRPV1 levels and maintains heat hyperalgesia. *Neuron* **36**:57–68. DOI: https://doi.org/10.1016/S0896-6273(02)00908-X, PMID: 12367506

Ji RR, Xu ZZ, Gao YJ. 2014. Emerging targets in neuroinflammation-driven chronic pain. *Nature Reviews. Drug Discovery* **13**:533–548. DOI: https://doi.org/10.1038/nrd4334, PMID: 24948120

Jie P, Hong Z, Tian Y, Li Y, Lin L, Zhou L, Du Y, Chen L, Chen L.. e 2015. Activation of transient receptor potential vanilloid 4 induces apoptosis in hippocampus through downregulating PI3K/Akt and upregulating p38

MAPK signaling pathways. *Cell Death & Disease* **6**:e1775. DOI: https://doi.org/10.1038/cddis.2015.146, PMID: 26043075

Johannes CB, Le TK, Zhou X, Johnston JA, Dworkin RH. 2010. The prevalence of chronic pain in United States adults: results of an Internet-based survey. *The Journal of Pain* **11**:1230–1239. DOI: https://doi.org/10.1016/j.jpain.2010.07.002, PMID: 20797916

Katanosaka Y, Iwasaki K, Ujihara Y, Takatsu S, Nishitsuji K, Kanagawa M, Sudo A, Toda T, Katanosaka K, Mohri S, Naruse K. 2014. TRPV2 is critical for the maintenance of cardiac structure and function in mice. *Nature Communications* **5**:3932. DOI: https://doi.org/10.1038/ncomms4932, PMID: 24874017

Keh SM, Facer P, Simpson KD, Sandhu G, Saleh HA, Anand P. 2008. Increased nerve fiber expression of sensory sodium channels Nav1.7, Nav1.8, And Nav1.9 in rhinitis. *The Laryngoscope* **118**:573–579. DOI: https://doi.org/10.1097/MLG.0b013e3181625d5a, PMID: 18197135

Kohn AD, Kovacina KS, Roth RA. 1995. Insulin stimulates the kinase activity of RAC-PK, a pleckstrin homology domain containing ser/thr kinase. *The EMBO Journal* **14**:4288–4295. DOI: https://doi.org/10.1002/j.1460-2075.1995.tb00103.x, PMID: 7556070

Kozik A, Moore RB, Potempa J, Imamura T, Rapala-Kozik M, Travis J. 1998. A novel mechanism for bradykinin production at inflammatory sites. Diverse effects of a mixture of neutrophil elastase and mast cell tryptase versus tissue and plasma kallikreins on native and oxidized kininogens. *The Journal of Biological Chemistry* **273**:33224–33229. DOI: https://doi.org/10.1074/jbc.273.50.33224, PMID: 9837892

Lardner A. 2001. The effects of extracellular pH on immune function. *Journal of Leukocyte Biology* **69**:522–530. DOI: https://doi.org/10.1189/jlb.69.4.522, PMID: 11310837

Lee KF, Li E, Huber LJ, Landis SC, Sharpe AH, Chao MV, Jaenisch R. 1992. Targeted mutation of the gene encoding the low affinity NGF receptor p75 leads to deficits in the peripheral sensory nervous system. *Cell* **69**:737–749. DOI: https://doi.org/10.1016/0092-8674(92)90286-L, PMID: 1317267

Lemmon MA. 2008. Membrane recognition by phospholipid-binding domains. *Nature Reviews Molecular Cell Biology* **9**:99–111. DOI: https://doi.org/10.1038/nrm2328, PMID: 18216767

Malek M, Kielkowska A, Chessa T, Anderson KE, Barneda D, Pir P, Nakanishi H, Eguchi S, Koizumi A, Sasaki J, Juvin V, Kiselev VY, Niewczas I, Gray A, Valayer A, Spensberger D, Imbert M, Felisbino S, Habuchi T, Beinke S, et al. 2017. PTEN Regulates PI(3,4)P_2 Signaling Downstream of Class I PI3K. *Molecular Cell* **68**:566–580. DOI: https://doi.org/10.1016/j.molcel.2017.09.024, PMID: 29056325

Mattheyses AL, Axelrod D. 2006. Direct measurement of the evanescent field profile produced by objective-based total internal reflection fluorescence. *Journal of Biomedical Optics* **11**:014006. DOI: https://doi.org/10.1117/1.2161018, PMID: 16526883

Mcmahon SB, Bennett DLH, Priestley JV, Shelton DL. 1995. The biological effects of endogenous nerve growth factor on adult sensory neurons revealed by a trkA-IgG fusion molecule. *Nature Medicine* **1**:774–780. DOI: https://doi.org/10.1038/nm0895-774

Mercado J, Gordon-Shaag A, Zagotta WN, Gordon SE. 2010. Ca2+-dependent desensitization of TRPV2 channels is mediated by hydrolysis of phosphatidylinositol 4,5-bisphosphate. *Journal of Neuroscience* **30**:13338–13347. DOI: https://doi.org/10.1523/JNEUROSCI.2108-10.2010, PMID: 20926660

Miled N, Yan Y, Hon WC, Perisic O, Zvelebil M, Inbar Y, Schneidman-Duhovny D, Wolfson HJ, Backer JM, Williams RL. 2007. Mechanism of two classes of cancer mutations in the phosphoinositide 3-kinase catalytic subunit. *Science* **317**:239–242. DOI: https://doi.org/10.1126/science.1135394, PMID: 17626883

Morenilla-Palao C, Planells-Cases R, García-Sanz N, Ferrer-Montiel A. 2004. Regulated exocytosis contributes to protein kinase C potentiation of vanilloid receptor activity. *Journal of Biological Chemistry* **279**:25665–25672. DOI: https://doi.org/10.1074/jbc.M311515200, PMID: 15066994

Perálvarez-Marín A, Doñate-Macian P, Gaudet R. 2013. What do we know about the transient receptor potential vanilloid 2 (TRPV2) ion channel? *FEBS Journal* **280**:5471–5487. DOI: https://doi.org/10.1111/febs.12302, PMID: 23615321

Raffioni S, Bradshaw RA. 1992. Activation of phosphatidylinositol 3-kinase by epidermal growth factor, basic fibroblast growth factor, and nerve growth factor in PC12 pheochromocytoma cells. *PNAS* **89**:9121–9125. DOI: https://doi.org/10.1073/pnas.89.19.9121, PMID: 1384043

Rahaman SO, Grove LM, Paruchuri S, Southern BD, Abraham S, Niese KA, Scheraga RG, Ghosh S, Thodeti CK, Zhang DX, Moran MM, Schilling WP, Tschumperlin DJ, Olman MA. 2014. TRPV4 mediates myofibroblast differentiation and pulmonary fibrosis in mice. *Journal of Clinical Investigation* **124**:5225–5238. DOI: https://doi.org/10.1172/JCI75331, PMID: 25365224

Rasband WS. 1997. *Image J.U.S. National Institute of Health*. Maryland: Scientific research an academic publisher.

Reichhart N, Keckeis S, Fried F, Fels G, Strauss O. 2015. Regulation of surface expression of TRPV2 channels in the retinal pigment epithelium. *Graefe's Archive for Clinical and Experimental Ophthalmology* **253**:865–874. DOI: https://doi.org/10.1007/s00417-014-2917-7, PMID: 25616727

Sarbassov DD, Guertin DA, Ali SM, Sabatini DM. 2005. Phosphorylation and regulation of Akt/PKB by the rictor-mTOR complex. *Science* **307**:1098–1101. DOI: https://doi.org/10.1126/science.1106148, PMID: 15718470

Sharma S, Goswami R, Merth M, Cohen J, Lei KY, Zhang DX, Rahaman SO. 2017. TRPV4 ion channel is a novel regulator of dermal myofibroblast differentiation. *American Journal of Physiology-Cell Physiology* **312**:C562–C572. DOI: https://doi.org/10.1152/ajpcell.00187.2016, PMID: 28249987

Shu X, Mendell LM. 1999. Nerve growth factor acutely sensitizes the response of adult rat sensory neurons to capsaicin. *Neuroscience Letters* **274**:159–162. DOI: https://doi.org/10.1016/S0304-3940(99)00701-6, PMID: 10548414

Songyang Z, Shoelson SE, Chaudhuri M, Gish G, Pawson T, Haser WG, King F, Roberts T, Ratnofsky S, Lechleider RJ. 1993. SH2 domains recognize specific phosphopeptide sequences. *Cell* **72**:767–778. DOI: https://doi.org/10.1016/0092-8674(93)90404-E, PMID: 7680959

Stein AT, Ufret-Vincenty CA, Hua L, Santana LF, Gordon SE. 2006. Phosphoinositide 3-kinase binds to TRPV1 and mediates NGF-stimulated TRPV1 trafficking to the plasma membrane. *The Journal of General Physiology* **128**: 509–522. DOI: https://doi.org/10.1085/jgp.200609576, PMID: 17074976

Stokoe D, Stephens LR, Copeland T, Gaffney PR, Reese CB, Painter GF, Holmes AB, McCormick F, Hawkins PT. 1997. Dual role of phosphatidylinositol-3,4,5-trisphosphate in the activation of protein kinase B. *Science* **277**: 567–570. DOI: https://doi.org/10.1126/science.277.5325.567, PMID: 9228007

Strotmann R, Schultz G, Plant TD. 2003. Ca2+-dependent potentiation of the nonselective cation channel TRPV4 is mediated by a C-terminal calmodulin binding site. *The Journal of Biological Chemistry* **278**:26541–26549. DOI: https://doi.org/10.1074/jbc.M302590200, PMID: 12724311

Suh YG, Oh U. 2005. Activation and activators of TRPV1 and their pharmaceutical implication. *Current Pharmaceutical Design* **11**:2687–2698. DOI: https://doi.org/10.2174/1381612054546789, PMID: 16101449

Sun R, Yan J, Willis WD. 2007. Activation of protein kinase B/Akt in the periphery contributes to pain behavior induced by capsaicin in rats. *Neuroscience* **144**:286–294. DOI: https://doi.org/10.1016/j.neuroscience.2006.08.084, PMID: 17084039

Tanaka Y, Niwa S, Dong M, Farkhondeh A, Wang L, Zhou R, Hirokawa N. 2016. The Molecular Motor KIF1A Transports the TrkA neurotrophin receptor and is essential for sensory neuron survival and function. *Neuron* **90**: 1215–1229. DOI: https://doi.org/10.1016/j.neuron.2016.05.002, PMID: 27263974

Thakor DK, Lin A, Matsuka Y, Meyer EM, Ruangsri S, Nishimura I, Spigelman I. 2009. Increased peripheral nerve excitability and local NaV1.8 mRNA up-regulation in painful neuropathy. *Molecular Pain* **5**:1744-8069-5-14. DOI: https://doi.org/10.1186/1744-8069-5-14, PMID: 19320998

Tissot M, Strzalko S, Thuret A, Giroud JP. 1989. Prostanoid release by macrophages at a distance from an inflammatory site. *British Journal of Experimental Pathology* **70**:525–531. PMID: 2818931

Toettcher JE, Gong D, Lim WA, Weiner OD. 2011. Light-based feedback for controlling intracellular signaling dynamics. *Nature Methods* **8**:837–839. DOI: https://doi.org/10.1038/nmeth.1700, PMID: 21909100

Trebino CE, Stock JL, Gibbons CP, Naiman BM, Wachtmann TS, Umland JP, Pandher K, Lapointe JM, Saha S, Roach ML, Carter D, Thomas NA, Durtschi BA, McNeish JD, Hambor JE, Jakobsson PJ, Carty TJ, Perez JR, Audoly LP. 2003. Impaired inflammatory and pain responses in mice lacking an inducible prostaglandin E synthase. *PNAS* **100**:9044–9049. DOI: https://doi.org/10.1073/pnas.1332766100, PMID: 12835414

Ufret-Vincenty CA, Klein RM, Collins MD, Rosasco MG, Martinez GQ, Gordon SE. 2015. Mechanism for phosphoinositide selectivity and activation of TRPV1 ion channels. *The Journal of General Physiology* **145**:431–442. DOI: https://doi.org/10.1085/jgp.201511354, PMID: 25918361

Vanhaesebroeck B, Guillermet-Guibert J, Graupera M, Bilanges B. 2010. The emerging mechanisms of isoform-specific PI3K signalling. *Nature Reviews Molecular Cell Biology* **11**:329–341. DOI: https://doi.org/10.1038/nrm2882, PMID: 20379207

Várnai P, Bondeva T, Tamás P, Tóth B, Buday L, Hunyady L, Balla T. 2005. Selective cellular effects of overexpressed pleckstrin-homology domains that recognize PtdIns(3,4,5)P3 suggest their interaction with protein binding partners. *Journal of Cell Science* **118**:4879–4888. DOI: https://doi.org/10.1242/jcs.02606, PMID: 16219693

Vetter ML, Martin-Zanca D, Parada LF, Bishop JM, Kaplan DR. 1991. Nerve growth factor rapidly stimulates tyrosine phosphorylation of phospholipase C-gamma 1 by a kinase activity associated with the product of the trk protooncogene. *PNAS* **88**:5650–5654. DOI: https://doi.org/10.1073/pnas.88.13.5650, PMID: 1712104

Willis WJ. 1978. *Sensory Mechanisms of the Spinal Cord*. New York: Springer.

Xu JT, Tu HY, Xin WJ, Liu XG, Zhang GH, Zhai CH. 2007. Activation of phosphatidylinositol 3-kinase and protein kinase B/Akt in dorsal root ganglia and spinal cord contributes to the neuropathic pain induced by spinal nerve ligation in rats. *Experimental Neurology* **206**:269–279. DOI: https://doi.org/10.1016/j.expneurol.2007.05.029, PMID: 17628541

Xu Q, Fitzsimmons B, Steinauer J, O'Neill A, Newton AC, Hua XY, Yaksh TL. 2011. Spinal phosphinositide 3-kinase-Akt-mammalian target of rapamycin signaling cascades in inflammation-induced hyperalgesia. *Journal of Neuroscience* **31**:2113–2124. DOI: https://doi.org/10.1523/JNEUROSCI.2139-10.2011, PMID: 21307248

Zhang X, Huang J, McNaughton PA. 2005. NGF rapidly increases membrane expression of TRPV1 heat-gated ion channels. *The EMBO Journal* **24**:4211–4223. DOI: https://doi.org/10.1038/sj.emboj.7600893